

# Ground-state landscape of 2d $\pm J$ Ising spin glasses

Alexander K. Hartmann

hartmann@theorie.physik.uni-goettingen.de

Institut für theoretische Physik, Heidelberg, Germany  
and

Institut für theoretische Physik, Bunsenstr. 9  
37073 Göttingen, Germany\*  
Tel. +49-551-399568, Fax. +49-551-399631  
(May 26, 2022)

Large numbers of ground states of two-dimensional Ising spin glasses with periodic boundary conditions in both directions are calculated for sizes up to  $40^2$ . A combination of a genetic algorithm and Cluster-Exact Approximation is used. For each quenched realization of the bonds up to 40 independent ground states are obtained.

For the infinite system a ground-state energy of  $e = -1.4015(3)$  is extrapolated. The ground-state landscape is investigated using a finite-size scaling analysis of the distribution of overlaps. The mean-field picture assuming a complex landscape describes the situation better than the droplet-scaling model, where for the infinite system mainly two ground states exist. Strong evidence is found that the ground states are not organized in an ultrametric fashion in contrast to previous results for three-dimensional spin glasses.

*Introduction* In this work two-dimensional Edwards-Anderson (EA)  $\pm J$  spin glasses [1] are investigated. They consist of  $N$  spins  $\sigma_i = \pm 1$ , described by the Hamiltonian

$$H \equiv - \sum_{\langle i,j \rangle} J_{ij} \sigma_i \sigma_j \quad (1)$$

The spins are placed on a two-dimensional ( $d=2$ ) square lattice of linear size  $L$  with periodic boundary conditions in both directions. Systems with quenched disorder of the nearest-neighbor interactions (bonds) are investigated. Their possible values are  $J_{ij} = \pm 1$  with equal probability. A constraint is imposed, so that  $\sum_{\langle i,j \rangle} J_{ij} = 0$ .

A question which has led to much controversy is, whether many pure states exist for finite dimensional, i.e. realistic spin glasses. For the infinite ranged Sherrington-Kirkpatrick (SK) Ising spin glass [2] this question was answered positively by the replica-symmetry-breaking mean-field (MF) scheme by Parisi [3]. Additionally this solution of the SK-model exhibits [4,5] an *ultrametric* structure: The distances  $d^{\alpha\beta}$  between the states do not only satisfy the triangular inequality  $d^{\alpha\beta} \leq d^{\alpha\gamma} + d^{\gamma\beta}$  but

the stronger ultrametric inequality  $d^{\alpha\beta} \leq \max(d^{\alpha\gamma}, d^{\gamma\beta})$  as well. For an introduction to ultrametricity see [6]. Numerical work on the subject for the SK-model can be found in [7,8].

A complete different model is proposed by the Droplet Scaling (DS) theory [9-13]. It suggests that only two pure states (related by a global flip) exist and that the most relevant excitations are obtained by reversing large domains of spins (the droplets). Some authors [14] disbelieve that the MF theory is consistent for realistic spin glasses but the question about the existence of many pure states is not answered.

In this work the point is not addressed by investigating spin glasses at finite temperature, but a different approach is used: an analysis of ground states is performed. The existence of many pure states implies that between two ground-state configurations arbitrary differences are possible. Otherwise two ground states would only differ by the spin orientations in some finite domains, which is always possible in the  $\pm J$  model because of the discrete structure of the interaction distribution. Such a simple structure was found for example for the 3d random-field Ising model [15]. An investigation whether the ordering of the ground states is ultrametric is of interest on its own: it is conjectured that an ultrametric structure prohibits that the usual cluster algorithms for simulating a system at *finite temperature* work efficiently [16].

Next a short overview about numerical results of finite-dimensional systems for investigating the low-temperature behavior are given. In four dimensions the MF picture is well established. Even numerical evidence for ultrametricity at finite temperature but below the transition temperature  $T_G$  was found [17,18].

For three-dimensional systems recently evidences for the validity of some basic features of the MF picture were found using simulations at finite temperature [19] and ground-state calculations [20]. First attempts to find ultrametricity by simulation at finite temperature are given in [21,22]. Evidences for an ultrametric ground-state landscape of 3d systems were recently found [23].

The higher-dimensional systems exhibit a spin-glass phase at nonzero temperature [24,25], but the 2d model orders only at  $T = 0$  [26]. So the question arises whether it is possible to detect this difference in the structures of the ground-state landscape as well. Several results us-

---

\*present address

ing direct calculations of ground states of 2d spin glasses using approximation methods are known [27–32]. Also exact ground-states up to  $L = 50$  have been analyzed [26,33]. But in all these studies only one ground state per realization was calculated, so it was not possible to study the structure of degeneracy. First attempts of the calculation of many different ground states can be found in [34,35].

In the present study many different and independent true ground states of 2d  $\pm J$  spin glasses are examined in detail. A combination of a genetic algorithm [36,37] and *Cluster-Exact Approximation* (CEA) [35] is used. Recently it has been shown that this method is able to calculate true ground states of spin glasses [25]. Since true ground states are calculated directly, one does not encounter ergodicity problems or critical slowing down like in algorithms which base on Monte-Carlo methods. The ground-state landscape is investigated and it is discussed whether the MF or the DS picture describes its structure better. Also the ground states are analyzed whether they are ordered in an ultrametric fashion.

The paper is organized as follows: at first the algorithm used here for the calculation of the ground states is explained. Next all observables are defined. Then the results are presented. In the last section a conclusion is driven.

## ALGORITHM

For readers not familiar with the calculation of spin-glass ground states now a short introduction to the subject and a description of the algorithm used here are given. A detailed overview can be found in [38]

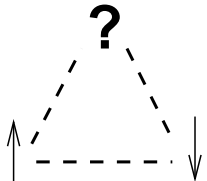


FIG. 1. The simplest frustrated system: a triple of spins, each pair of spins connected by antiferromagnetic bonds (dashed lines). It is not possible to satisfy all bonds.

The concept of *frustration* [39] is important for understanding the behavior of  $\pm J$  Ising spin glasses. The simplest example of a frustrated system is a triple of spins where all pairs are connected by antiferromagnetic bonds, see fig. 1. A bond is called *satisfied* if it contributes with a negative value to the total energy by choosing the values of its adjacent spins properly. For the triangle it is not possible to find a spin-configuration were all bonds are satisfied. In general a system is frustrated if closed loops of bonds exists, where the product of these bond-values is negative. For square and cubic systems the smallest

closed loops consist of four bonds. They are called (elementary) *plaquettes*.

As we will see later the presence of frustration makes the calculation of exact ground states of such systems computationally hard. Only for the special case of the two-dimensional system with periodic boundary conditions in no more than one direction and without external field a polynomial-time algorithm is known [40]. Now for the general case three basic methods are briefly reviewed and the largest system sizes which can be treated are given for three-dimensional systems, the standard spin-glass model.

The simplest method works by enumerating all  $2^N$  possible states and has obviously an exponential running time. Even a system size of  $4^3$  is too large. The basic idea of the so called *Branch-and-Bound* algorithm [41] is to exclude the parts of the state space, where no low-lying states can be found, so that the complete low-energy landscape of systems of size  $4^3$  can be calculated [42].

A more sophisticated method called *Branch-and-Cut* [43,33] works by rewriting the quadratic energy function as a linear function with an additional set of inequalities which must hold for the feasible solutions. Since not all inequalities are known a priori the method iteratively solves the linear problem, looks for inequalities which are violated, and adds them to the set until the solution is found. Since the number of inequalities grows exponentially with the system size the same holds for the computation time of the algorithm. With Branch-and-Cut anyway small systems up to  $8^3$  are feasible.

The method used here is able to calculate true ground states [25] up to size  $14^3$ . For two-dimensional systems sizes up to  $50^2$  can be treated. This is about the same size Branch-and-Cut can solve, but in contrast to that method the algorithm used here is able to calculate many independent ground states for each realization of the randomness. The method bases on a special genetic algorithm [36,37] and on Cluster-Exact Approximation [35]. CEA is an optimization method designed specially for spin glasses. Its basic idea is to transform the spin glass in a way that graph-theoretical methods can be applied, which work only for systems exhibiting no frustrations. Next a description of the genetic CEA is given.

Genetic algorithms are biologically motivated. An optimal solution is found by treating many instances of the problem in parallel, keeping only better instances and replacing bad ones by new ones (survival of the fittest). The genetic algorithm starts with an initial population of  $M_i$  randomly initialized spin configurations (= *individuals*), which are linearly arranged using an array. The last one is also neighbor of the first one. Then  $n_o \times M_i$  times two neighbors from the population are taken (called *parents*) and two new configurations called *offsprings* are created. For that purpose the *triadic crossover* is used which turned out to be very efficient for spin glasses: a mask is used which is a third randomly chosen (usually distant) member of the population with a fraction of 0.1

of its spins reversed. In a first step the offsprings are created as copies of the parents. Then those spins are selected, where the orientations of the first parent and the mask agree [44]. The values of these spins are swapped between the two offsprings. Then a *mutation* with a rate of  $p_m$  is applied to each offspring, i.e. a fraction  $p_m$  of the spins is reversed.

Next for both offsprings the energy is reduced by applying CEA: The method constructs iteratively and randomly a non-frustrated cluster of spins. Spins adjacent to many unsatisfied bonds are more likely to be added to the cluster. During the construction of the cluster a local gauge-transformation of the spin variables is applied so that all interactions between cluster spins become ferromagnetic.

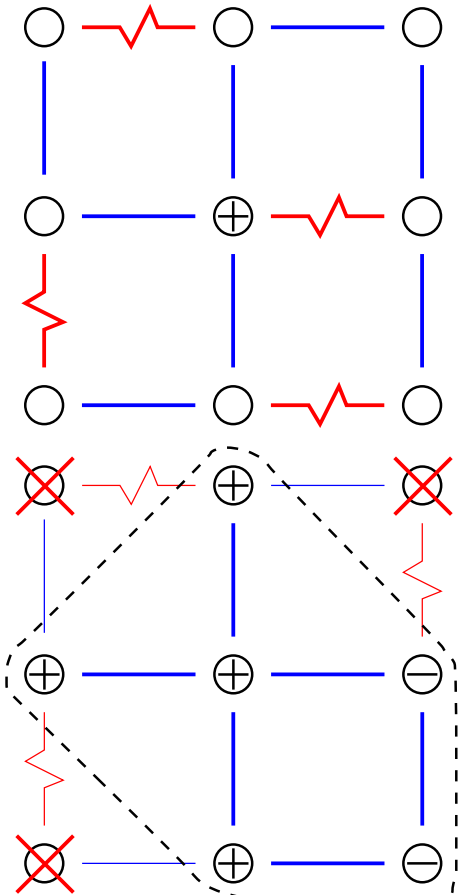


FIG. 2. Example of the Cluster-Exact Approximation method. A part of a spin glass is shown. The circles represent lattice sites/spins. Straight lines represent ferromagnetic bonds the jagged lines antiferromagnetic interactions. The top part shows the initial situation. The construction starts with the spin at the center. The bottom part displays the final stage. The spins which belong to the cluster carry a plus or minus sign which indicates how each spin is transformed, so that only ferromagnetic interactions remain inside the cluster. All other spins cannot be added to the cluster because it is not possible to multiply them by  $\pm 1$  to make all adjacent bonds positive. Please note that many other combinations of spins can be used to build a cluster without frustration.

Fig. 2 shows an example of how the construction of the cluster works using a small spin-glass system. For 2d  $\pm J$  spin glasses each cluster contains typically 70 percent of all spins. The non-cluster spins act like local magnetic fields on the cluster spins, so the ground state of the cluster is not trivial. Since the cluster has only ferromagnetic interactions, an energetic minimum state for its spins can be calculated in polynomial time by using graph theoretical methods [45–47]: an equivalent network is constructed [48], the maximum flow is calculated [49,50]<sup>1</sup> and the spins of the cluster are set to their orientations leading to a minimum in energy. This minimization step is performed  $n_{\min}$  times for each offspring.

Afterwards each offspring is compared with one of its parents. The pairs are chosen in the way that the sum of the phenotypic differences between them is minimal. The phenotypic difference is defined here as the number of spins where the two configurations differ. Each parent is replaced if its energy is not lower (i.e. not better) than the corresponding offspring. After this whole step is done  $n_o \times M_i$  times, the population is halved: From each pair of neighbors the configuration which has the higher energy is eliminated. If more than 4 individuals remain the process is continued otherwise it is stopped and the best individual is taken as result of the calculation.

The representation in fig. 3 summarizes the algorithm.

The whole algorithm is performed  $n_R$  times and all configurations which exhibit the lowest energy are stored, resulting in  $n_G$  statistically independent ground-state configurations.

This algorithm was already applied to examine the ground-state landscape of 3d spin glasses [20].

<sup>1</sup>Implementation details: We used Tarjan's wave algorithm together with the heuristic speed-ups of Träff. In the construction of the *level graph* we allowed not only edges  $(v, w)$  with  $\text{level}(w) = \text{level}(v)+1$ , but also all edges  $(v, t)$  where  $t$  is the sink. For this measure, we observed an additional speed-up of roughly factor 2 for the systems we calculated.

```

algorithm genetic CEA( $\{J_{ij}\}$ ,  $M_i$ ,  $n_o$ ,  $p_m$ ,  $n_{\min}$ )
begin
  create  $M_i$  configurations randomly
  while ( $M_i > 4$ ) do
    begin
      for  $i = 1$  to  $n_o \times M_i$  do
        begin
          select two neighbors
          create two offsprings using triadic crossover
          do mutations with rate  $p_m$ 
          for both offsprings do
            begin
              for  $j = 1$  to  $n_{\min}$  do
                begin
                  construct unfrustrated cluster of spins
                  construct equivalent network
                  calculate maximum flow
                  construct minimum cut
                  set new orientations of cluster spins
                end
                if offspring is not worse than related parent
                then
                  replace parent with offspring
                end
              end
            end
          end
          half population;  $M_i = M_i/2$ 
        end
      return one configuration with lowest energy
    end

```

FIG. 3. Genetic Cluster-exact Approximation.

## OBSERVABLES

For a fixed realization  $J = \{J_{ij}\}$  of the exchange interactions and two replicas  $\{\sigma_i^\alpha\}, \{\sigma_i^\beta\}$ , the overlap [3] is defined as

$$q^{\alpha\beta} \equiv \frac{1}{N} \sum_i \sigma_i^\alpha \sigma_i^\beta \quad (2)$$

The ground state of a given realization is characterized by the probability density  $P_J(q)$ . Averaging over the realizations  $J$ , denoted by  $[\cdot]_{av}$ , results in ( $Z$  = number of realizations)

$$P(q) \equiv [P_J(q)]_{av} = \frac{1}{Z} \sum_J P_J(q) \quad (3)$$

The probability densities are symmetric as no external field is applied:  $P_J(q) = P_J(-q)$  and  $P(q) = P(-q)$ . Hence, only averages of  $|q|^n$  are relevant:

$$\overline{|q_J|^n} \equiv \int_{-1}^1 |q|^n P_J(q) dq \quad (4)$$

$$\overline{|q|^n} \equiv \int_{-1}^1 |q|^n P(q) dq \quad (5)$$

The Droplet model predicts that only two pure states exist, implying that  $P(q)$  converges for  $L \rightarrow \infty$  to  $P(q) = \frac{1}{2}(\delta(q - q_{EA}) + \delta(q + q_{EA}))$ , while in the MF picture the density remains nonzero for a range  $-q_{EA} \leq q \leq q_{EA}$  with peaks at  $\pm q_{\max}$  ( $0 < q_{\max} \leq q_{EA}$ ,  $q_{\max} \rightarrow q_{EA}$  for  $L \rightarrow \infty$ ). Consequently the variance

$$\sigma^2(|q|) \equiv \int_{-1}^1 (\overline{|q|} - |q|)^2 P(q) dq = \overline{|q|^2} - \overline{|q|}^2 \quad (6)$$

stays finite for  $L \rightarrow \infty$  in the MF pictures ( $\sigma^2(|q|) = s_\infty + s_1/L^{s_2}$ ) [51], while  $\sigma^2(|q|) \sim L^{-y} \rightarrow 0$  according the DS approach. Here,  $y$  is the zero-temperature scaling exponent [9], which is denoted as  $\Theta$  in [11,12].

Another way of describing the finite-size behavior of  $P(|q|)$  is to sum up the contributions from small overlap-values  $q \leq q_0$ :

$$X_{q_0} \equiv \int_{-q_0}^{q_0} P(q) dq \quad (7)$$

This value should converge to 0 in the DS picture as long as  $q_0 < q_{EA}$  while it should stay non-zero for the MF framework.

The overlap defined in (2) can be used to measure the distance  $d^{\alpha\beta}$  between two states:

$$d^{\alpha\beta} \equiv 0.5(1 - q^{\alpha\beta}) \quad (8)$$

with  $0 \leq d^{\alpha\beta} \leq 1$ . For three replicas  $\alpha, \beta, \gamma$  the usual triangular inequality reads  $d^{\alpha\beta} \leq d^{\alpha\gamma} + d^{\gamma\beta}$ . Written in terms of  $q$  it becomes

$$q^{\alpha\beta} \geq q^{\alpha\gamma} + q^{\gamma\beta} - 1 \quad (9)$$

In an *ultrametric* space [6] the triangular inequality is replaced by a stronger one  $d^{\alpha\beta} \leq \max(d^{\alpha\gamma}, d^{\gamma\beta})$  or equivalently

$$q^{\alpha\beta} \geq \min(q^{\alpha\gamma}, q^{\gamma\beta}) \quad (10)$$

An example of an ultrametric space is the set of leaves of a binary tree: the distance between two leaves is defined by the number of edges on a path between the leaves.

Let  $q_1 \leq q_2 \leq q_3$  be the overlaps  $q^{\alpha\beta}, q^{\alpha\gamma}, q^{\gamma\beta}$  ordered according their sizes. By writing the smallest overlap on the left side in equation (10), one realizes that two of the overlaps must be equal and the third may be larger or the same:  $q_1 = q_2 \leq q_3$

In a finite-size system this relation may be violated. Here two ways are used of determining whether ground states of realistic spin glasses become more and more ultrametric with increasing size  $L$ :

- The difference

$$\delta q \equiv q_2 - q_1 \quad (11)$$

is calculated for all triplets. Because the influence of the absolute size of the overlaps should be excluded the third overlap is fixed:  $q_3 = q_{fix}$ . In practice only overlap triples are used where  $q_3 \in [q_{fix}, q_{fix2}]$  holds to obtain sufficient statistics. With increasing size  $L$  the distribution  $P(\delta q)$  should tend to a Dirac delta function for an ultrametric system [8].

- If two overlaps are fixed ( $q^{\alpha\gamma} = q^{\beta\gamma} = q_{fix}$ , in practice  $q^{\alpha\gamma}, q^{\beta\gamma} \in [q_{fix}, q_{fix2}]$ ), equation (9) implies  $q \equiv q^{\alpha\beta} \geq 2q_{fix} - 1$  while ultrametricity implies  $q \geq q_{fix}$  which is stronger if  $q_{fix} < 1$  [17]. The distribution  $P_{2-fix}(q)$  of the third overlap is used to characterize the ultrametricity of a system. Additionally the weighted fraction of the distribution outside  $[q_{fix}, q_{EA}]$

$$I_L \equiv \int_{-1}^{q_{fix}} P_{2-fix}(q)(q - q_{fix})^2 dq + \int_{q_{EA}}^1 P_{2-fix}(q)(q - q_{EA})^2 dq \quad (12)$$

(see [17]) should vanish for  $L \rightarrow \infty$  in an ultrametric system.

## RESULTS

We used simulation parameters determined in the following way: For each system size several different combinations of the parameters  $M_i, n_o, n_{min}, p_m$  were tested. For the final parameter sets it is not possible to obtain lower energies even by using parameters where the calculation consumes four times the computational effort. Using parameter sets chosen this way genetic CEA calculates true ground states, as shown in [25]. Here a mutation rate of  $p_m = 0.05$  and  $n_R = 40$  runs per realization were used for all system sizes. Table 1 summarizes the parameters and gives the typical computer time  $\tau$  spent per ground state computation on a 80 MHz PPC601. For each system size ground states for 1000 different realizations of the disorder were calculated. On average  $n_G > 29$  (not necessarily different) ground-state configurations were obtained for all system sizes  $L$  using  $n_R = 40$  runs per realization.

$L$	$M_i$	$n_o$	$n_{min}$	$\tau$ (sec)
5	8	1	1	0.02
10	16	1	2	0.4
14	16	4	2	3
20	32	8	2	30
32	128	8	2	780
40	512	8	2	5400

Tab 1. Simulation parameters:  $L$  = system size,  $M_i$  = initial size of population,  $n_o$  = average number of off-

springs per configuration,  $n_{min}$  = number of CEA minimization steps per offspring,  $\tau$  = average computer time per ground state on a 80MHz PPC601.

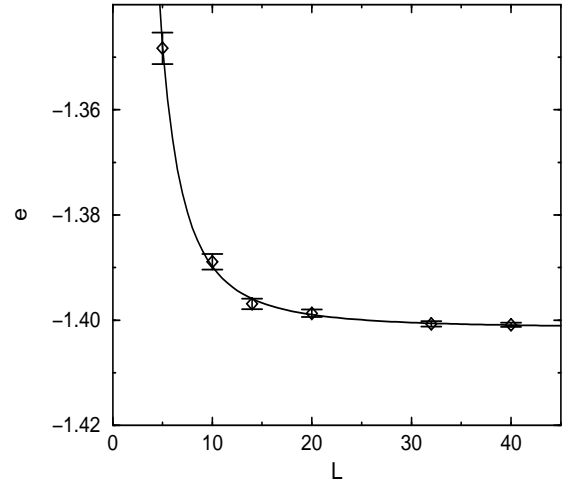


FIG. 4. Average ground-state energy of 2d  $\pm J$  Ising spin glass for linear dimensions  $5 \leq L \leq 40$  and FSS fit of form  $e(L) = e_\infty + e_1 L^{-e_2}$  resulting in  $e_\infty = -1.4015(3)$ .

At first the result for the ground-state energy as function of system size is presented in fig. 4. By performing a finite-size scaling (FSS) analysis using the function  $e(L) = e_\infty + e_1 L^{-e_2}$  a ground-state energy of the infinite system of  $e_\infty = -1.4015(3)$  is obtained. This is consistent with an extrapolation from exact ground states of finite systems  $e_\infty = -1.4015(8)$  [33] and with other former results from transfer-matrix calculations  $e_\infty = -1.402(1)$  [27], Monte-Carlo simulations  $e_\infty = -1.407(8)$  [28], multicanonical simulations  $e_\infty = -1.394(7)$  [30], genetic algorithms  $e_\infty = -1.400(5)$  [31],  $e_\infty = -1.401(1)$  [32], a special cluster-construction method  $e_\infty = -1.402(2)$  [29] and pure CEA  $e_\infty = -1.400(5)$  [35]. The value presented here has a higher accuracy than the former results.

The exponent of the decay is  $e_2 = 2.2(1)$  which is much larger than the upper limit of  $y \equiv e_2 \leq (d - 1)/2 = 0.5$  proposed by DS. This is an evidence that the DS picture may not be appropriate for 2d realistic spin glasses.

Information about the ground-state landscape can be extracted by evaluating the distribution of overlaps. In fig. 5  $P(|q|)$  is shown for three sample sizes  $L = 10, 20, 40$ . The distribution is averaged over the disorder, where each realization enters the result with the same weight, independent of the number of ground-state configurations which were available. The distributions extent over large intervals down to  $q = 0$  which indicates the existence of a complex ground-state landscape. For small overlaps no large change is visible with increasing system size, but the peak of the distributions located at larger  $q$ -values shifts to smaller values.

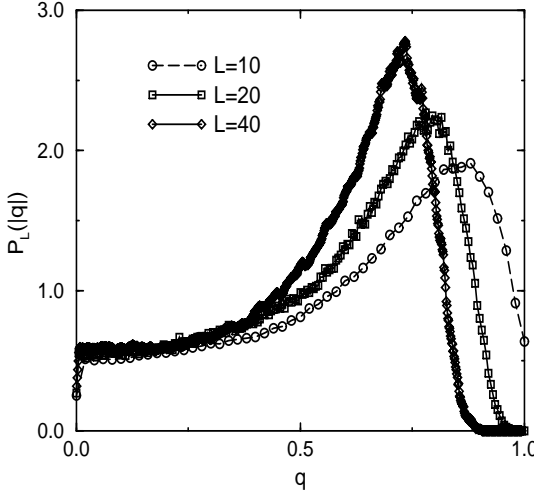


FIG. 5. Distribution of overlaps  $P(|q|)$  for ground states of  $2d \pm J$  Ising spin glass for  $L = 10, 20, 40$ . Only for large values of  $q$  a difference is visible, so even for large systems there is a finite probability of overlap  $q = 0$ . The lines are guides for the eyes only.

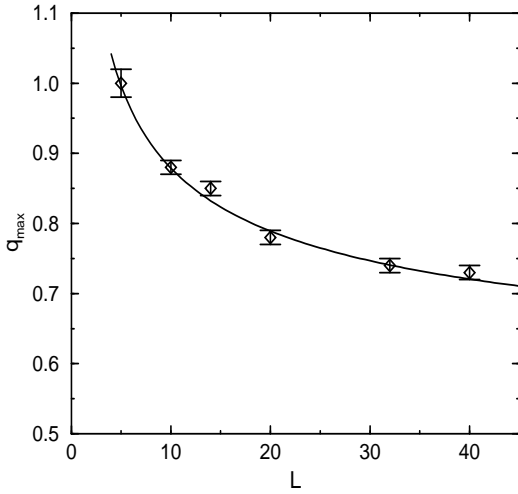


FIG. 6. Position  $q_{\max}$  of this peak can be used to calculate the Edwards-Anderson order parameter  $q_{EA}$  which is the maximum value of  $q$  where  $P(q)$  is nonzero in the infinite system. Fig. 6 shows the value of  $q_{\max}$  as function of  $L$ . Using a FSS fit with  $q_{\max}(L) = q_{EA} + q_1 L^{-q_2}$  a value of  $q_{EA} = 0.50(9)$  is obtained. The resulting function is shown in the figure using a line.

The position  $q_{\max}$  of this peak can be used to calculate the Edwards-Anderson order parameter  $q_{EA}$  which is the maximum value of  $q$  where  $P(q)$  is nonzero in the infinite system. Fig. 6 shows the value of  $q_{\max}$  as function of  $L$ . Using a FSS fit with  $q_{\max}(L) = q_{EA} + q_1 L^{-q_2}$  a value of  $q_{EA} = 0.50(9)$  is obtained. The resulting function is shown in the figure using a line.

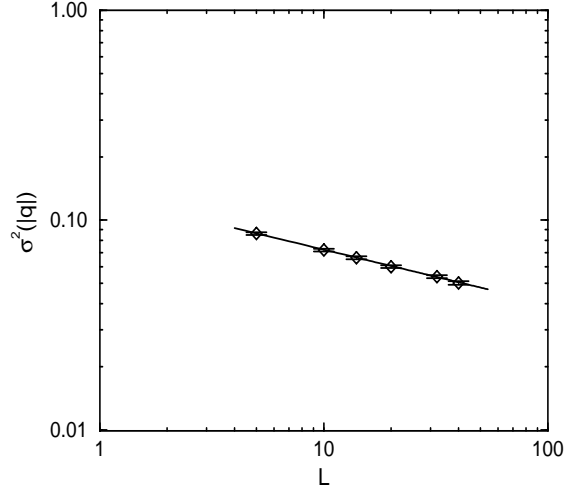


FIG. 7. Variances  $\sigma^2(|q|)$  of the distributions of overlaps  $P(|q|)$  as function of  $L$  for  $5 \leq L \leq 40$ . For  $L \rightarrow \infty$  the value converges to a small value. A fit of the form  $s_\infty + s_1 L^{-s_2}$  gives  $s_\infty = 0.004(8)$ . The straight line shows a fit with  $s_\infty \equiv 0$ , which should be true for a simple ground-state landscape.

So far we have seen that finite systems exhibit a complex ground-state landscape. But to decide whether this is true even for the infinite system one must investigate the shape of  $P(|q|)$  as function of system size  $L$ . In fig. 7 the variance (see def. (6)) of the distribution is shown as function of  $L$ . By fitting the variance to a function of form  $\sigma^2(L) = s_\infty + s_1 L^{-s_2}$  a value of  $s_\infty = 0.004(8)$  was obtained. This result is very close to zero. In the figure a fit with  $s_\infty \equiv 0$  is shown which looks very reasonable. So it is possible that for  $L \rightarrow \infty$  the width of the distribution shrinks to zero, which would mean that the ground-state landscape is simple, as described by the DS framework. This is different from the case of the three-dimensional model, where the same procedure resulted in  $s_\infty^{3d} = 0.0608(6)$  [20].

However, the impression mediating from fig. 5 is different: a long tail down to  $q = 0$  persists for all system sizes, so a width of zero for the infinite systems seems unlikely. Consider an infinite system, where the overlaps are distributed according a distribution with a constant probability-density of 0.5 for  $q \leq 0.5$  and a delta-function at  $q = 0.5$  with weight 0.75:  $P(q) = 0.25\Theta(0.5 - p) + 0.75\delta(p - 0.5)$  ( $p \geq 0$ ), which seems plausible from fig. 5 and 6. Then one obtains a variance  $\sigma^2(|q|) = 0.017$  which is very close to  $s_\infty$  regarding the given error-bar.

Since the result is not definite so far, next the contribution of small overlap-values to  $P(|q|)$  is studied. The fraction  $X_{q_0}$  (see def. (7)) of the distribution below a given value  $q_0$  is displayed in fig. 8 using  $q_0 \equiv 0.2 < 0.5 = q_{EA}$  as function of system size. As  $X_{q_0}$  seems to be independent of the system size it is reasonable to conclude that the infinite system has a broad distribution.

So far the question whether the ground-state landscape is complex has been addressed: a complex landscape for the 2d  $\pm J$  spin glass seems likely, but the results are less definite than earlier results for the 3d model.

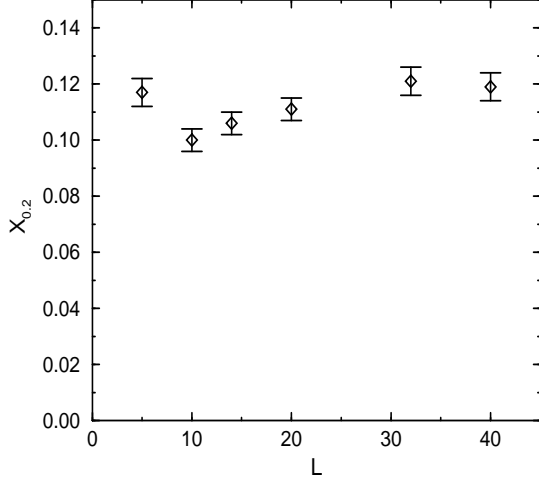


FIG. 8. Fraction  $X_{q_0}$  of the distributions of overlaps  $P(|q|)$  below  $q_0 = 0.2$  as function of  $L$  for  $5 \leq L \leq 40$ . The value of  $X_{0.2}$  does not decrease with growing  $L$  indicating a complex ground-state landscape.

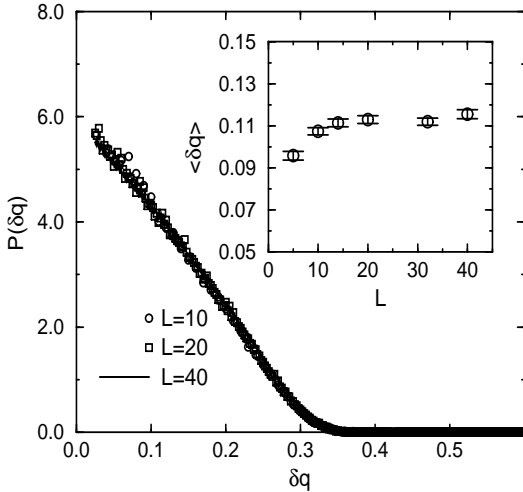


FIG. 9. Distribution  $P(\delta q)$  for different system sizes  $L = 10, 20, 40$  where  $\delta q = q_2 - q_1$  and  $q_1 \leq q_2 \leq q_3$  are triplets of absolute values of overlaps from independent triplets of ground states. Only triplets with  $q_3 \in [0.25, 0.35]$  are used. For an infinite ultrametric system  $\delta q = 0$  holds. The distribution turns out to be independent of the system size indicating the absence ultrametricity for the ground states. The inset shows the average value of  $\delta q$  as function of system size  $L$ .

In the second part of this section it is studied whether the ground states are ultrametrically ordered. For that purpose for each realization all possible triplets of ground states were chosen and the corresponding three overlaps evaluated. The quantity  $\delta q$  which is the difference between the two smaller overlap values was calculated (see equation (11)) for all possible triplets with a constraint for the largest of the three overlaps:  $q_3 \in [\frac{3}{5}q_{EA} - 0.05, \frac{3}{5}q_{EA} + 0.05] = [0.25, 0.35]$  (which implies  $\delta q < 0.35$  as well). For an ultrametric system the distribution of  $\delta q$  should be a delta function. To improve the statistics we used the absolute value of all overlaps. The distribution  $P(\delta q)$  is shown in fig. 9 for  $L = 10, 20, 40$ . Each realization enters the distribution with the same weight. One can see that the distribution is independent of the system size. The average value of  $\delta q$  as function of system size shown in the inset. Hence, in the infinite system  $\delta q > 0$  is possible. It seems that the 2d  $\pm J$  spin glass is not ultrametric, which is in strong contrast to the result for the three-dimensional model where  $P(\delta q)$  converges to a delta-function [23].

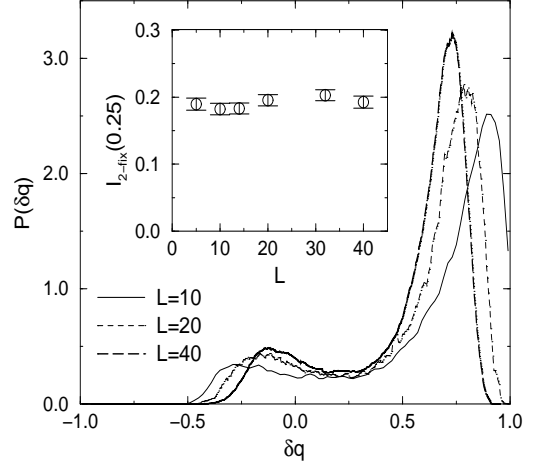


FIG. 10. Distribution  $P_{2-fix}(q)$  for different system sizes  $L = 10, 20, 40$  where  $q \in \{q_1, q_2, q_3\}$  and  $q_1 \leq q_2 \leq q_3$  are triplets of overlaps from independent triplets of ground states. Only  $q$ -values of triplets are used where the two other overlaps are within the interval  $[0.25, 0.35]$ . Then for an infinite ultrametric system  $q > 0.25$  should hold, while for a metric system just  $q > -0.5$  must hold. The small inset shows the value integrated from  $-1$  to  $0.25$ . With increasing system size the fraction of the distribution below  $0.25$  remains constant although the distribution itself changes. The lines are guides for the eyes only.

Additional information can be obtained by fixing two of the three overlaps of a triplet. We took all triplets where two arbitrary overlaps fell into the interval  $[\frac{3}{5}q_{EA} - 0.05, \frac{3}{5}q_{EA} + 0.05]$ . The resulting distributions  $P_{2-fix}(q)$  of the third remaining overlap is shown in fig. 10 for  $L = 10, 20, 40$ . The triangular inequality gives  $q > -0.5$  whereas for an ultrametric system  $q > 0.25$  must hold. We concentrate on the part of the distribution with  $q <$

0.25. Although the shape of the distribution changes a little bit, the fraction of the overlaps forbidden in an ultrametric system keeps fairly constant: the inset shows the fraction  $I_{2-fix}(0.25)$  of the distribution below  $q = 0.25$ . Again reasonable evidence against an ultrametric organization of the ground-states is found, but it is a little bit weaker, since very small values near  $q = -0.5$  disappear for large systems.

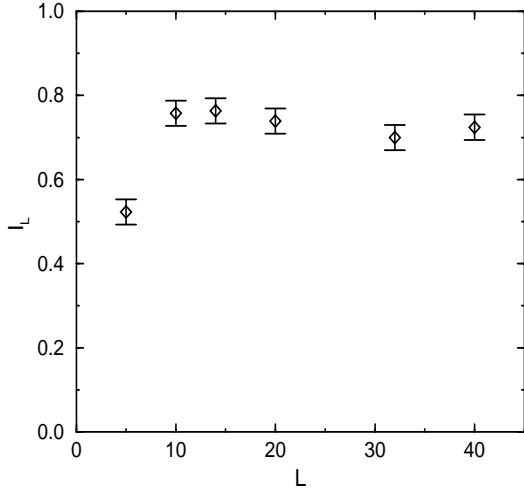


FIG. 11. Integrated value  $I_L$  of  $P_{2-fix}(q)$  outside  $[q_{fix}, q_{EA}]$  as function of system size  $L$  where  $q \in \{q_1, q_2, q_3\}$  and  $q_1 \leq q_2 \leq q_3$  are triples of overlaps from independent triples of ground states. Only  $q$ -values of triples where the two other overlaps are within the interval  $[0.25, 0.35]$  are used. With increasing system size the fraction of the distribution outside  $[0.25, 0.5]$  remains mainly constant, which indicates that 2d  $\pm J$  spin glasses are not ultrametric.

To complete the comparison with [23], the distribution  $P_{2-fix}(q)$  integrated outside  $[0.25, 0.5]$  (see def. of  $I_L$  in (13)) is shown in fig. 11. Again the result is different from the case of the three-dimensional  $\pm J$  spin glass: here  $I_L$  seems to remain non-zero for  $L \rightarrow \infty$ .

## CONCLUSION

Many different and independent ground states for 2d  $\pm J$  spin glasses were calculated up to sizes  $L = 40$  using the genetic Cluster-Exact Approximation. From former calculations and comparison with exact results is it clear that true ground states were obtained.

By evaluating the distribution of overlaps evidence for a complex organization of the ground states is found, but the evidence is weak, since it is not clear whether the width of the distribution of overlaps scales to zero with increasing system size. This is similar to the 3d case, but there the evidence for the MF picture is stronger.

By studying triplets of ground states with one or two of the three overlap values fixed convincing evidences are found that the ground states of 2d  $\pm J$  spin glasses are organized not in an ultrametric manner. This is very different from the three-dimensional model. To our opinion this may be connected with the fact that 3d realistic spin glasses have an ordered phase at finite temperature whereas the 2d model shows a spin-glass phase only at  $T = 0$ .

Since only moderate system sizes up to  $N = 40^2$  were investigated, the behavior might change at larger sizes. But the finite-size behavior of the data presented here is very smooth, thus, we believe that our results persist for  $L \rightarrow \infty$ .

The results presented here were obtained for a bimodal distribution of the interactions. For spin glasses with Gaussian distribution the ground state is unique, implying that  $P_L(|q|)$  are both the same in the MF and DS picture. The predictions are different at finite temperature. We expect the same behavior as for the  $\pm J$  model if one allows deviations of order one from the true ground-state energy, but for that system type ground states are much harder to calculate using the genetic CEA algorithm.

## ACKNOWLEDGEMENTS

The author thanks H. Horner and G. Reinelt for manifold support. He thanks K. Bhattacharya for critical reading of the manuscript and for giving many helpful hints. The author took much benefit from discussions with S. Kobe, H. Rieger and A.P. Young. He is also grateful to the *Paderborn Center for Parallel Computing* for the allocation of computer time. This work was supported by the Graduiertenkolleg “Modellierung und Wissenschaftliches Rechnen in Mathematik und Naturwissenschaften” at the *Interdisziplinäres Zentrum für Wissenschaftliches Rechnen* in Heidelberg.

---

- [1] For reviews on spin glasses see: K. Binder and A.P. Young, Rev. Mod. Phys. **58**, 801 (1986); M. Mézard, G. Parisi, M.A. Virasoro, *Spin glass theory and beyond*, World Scientific, Singapur 1987; K.H. Fisher and J.A. Hertz, *Spin Glasses*, Cambridge University Press, 1991;
- [2] D. Sherrington und S. Kirkpatrick, Phys. Rev. Lett. **35**, 1792-1796 (1975)
- [3] G. Parisi, Phys. Rev. Lett. 43, 1754 (1979); J. Phys. A 13, 1101 (1980); 13, 1887 (1980); 13, L115 (1980); Phys. Rev. Lett. 50, 1946 (1983).
- [4] M. Mézard, G. Parisi, N. Sourlas, G. Toulouse and M.A. Virasoro, Phys. Rev. Lett. **52**, 1156 (1984); J. de Phys. **45**, 843 (1984)

[5] S. Franz, G. Parisi and M.A. Virasoro, *Europhys. Lett.* **17**, 5 (1992); *J. de Phys. I* **2**, 1869 (1992)

[6] R. Rammal, G. Toulouse and M.A. Virasoro, *Rev. Mod. Phys.* **58**, 765 (1986)

[7] N. Parga, G. Parisi and M.A. Virasoro, *J. de Phys. Lett.* **45**, L1063 (1984)

[8] R.N. Bhatt and A.P. Young, *J. Mag. Mag. Mat.* **54-57**, 191 (1986)

[9] W.L. McMillan, *J. Phys. C* **17**, 3179 (1984).

[10] A.J. Bray and M.A. Moore, *J. Phys. C* **17**, L463 (1984); *J. Phys. C* **18**, L699 (1985).

[11] D.S. Fisher and D.A. Huse, *Phys. Rev. Lett.* **56**, 1601 (1986).

[12] D.S. Fisher and D.A. Huse, *Phys. Rev. B* **38**, 386 (1988).

[13] A. Bovier and J. Fröhlich, *J. Stat. Phys.* **44**, 347 (1986).

[14] C.M. Newman and D.L. Stein, *Phys. Rev. Lett.* **76**, 515 (1996)

[15] A.K. Hartmann, *Physica A* **248**, 1 (1998)

[16] N. Persky and S. Solomon, *Phys. Rev. E* **54**, 4399 (1996)

[17] A. Cacciuto, E. Marinari and G. Parisi, *J. Phys. A* **30**, L263 (1997)

[18] E. Marinari, G. Parisi and J.J. Ruiz-Lorenzo, in: *Spin Glasses and Random Fields*, Ed. A.P. Young, World Scientific 1998

[19] E. Marinari, G. Parisi, J. Ruiz-Lorenzo, F. Ritort, *Phys. Rev. Lett.* **76**, 843 (1996).

[20] A.K. Hartmann, *Europhys. Lett.* **40**, 429 (1997)

[21] N. Sourlas, *J. de Phys. Lett.* **45**, L969 (1984)

[22] S. Caracciolo, G. Parisi, S. Patarnello and N. Sourlas, *J. de Phys.* **51**, 1877 (1990)

[23] A.K. Hartmann, to appear in *Europhys. Lett.*, preprint cond-mat/9804325

[24] N. Kawashima and A.P. Young, *Phys. Rev. B* **53**, R484 (1996)

[25] A.K. Hartmann, to appear in *Phys. Rev. E*, preprint cond-mat/9806114

[26] N. Kawashima and H. Rieger, *Europhys. Lett.* **39**, 85 (1997)

[27] H.-F. Cheung and W.L. McMillan, *J. Phys. C* **16**, 7027 (1983)

[28] R.H. Swendson and J.S. Wang, *Phys. Rev. B* **38**, 4840 (1988)

[29] H. Freund and P. Grassberger, *J. Phys. A* **22**, 4045-4059 (1989)

[30] B.A. Berg and T. Celik, *Phys. Rev. Lett.* **69**, 2292 (1992); B.A. Berg, T. Celik and U. Hansmann, *Europhys. Lett.* **22**, 63 (1993); U.H.E. Hansmann and B.A. Berg, *Int. J. Mod. Phys. C* **5**, 263 (1994)

[31] P. Sutton, D.L. Hunter and N. Jan, *J. Physique I* **4**, 1281 (1994)

[32] U. Gropengiesser, *J. Stat. Phys.* **79**, 1005 (1995)

[33] C. De Simone, M. Diehl, M. Jünger, P. Mutzel, G. Reinelt and G. Rinaldi, *J. Stat. Phys.* **84**, 1363 (1996)  
*J. Stat. Phys.* **26**, 25 (1981)  
(1988)

[34] D. Stauffer and K. Binder, *Z. Phys. B* **30**, 313 (1978)

[35] A.K. Hartmann, *Physica A*, **224**, 480 (1996)

[36] K.F. Pál, *Physica A* **223**, 283 (1996)

[37] Z. Michalewicz, *Genetic Algorithms + Data Structures = Evolution Programs*, Springer, Berlin 1992

[38] H. Rieger, in: *Advances in Computer Simulation*, ed. J. Kertesz and I. Kondor, *Lecture Notes in Physics* **501**, (Springer-Verlag, Heidelberg, 1998)

[39] G. Toulouse, *Commun. Phys.* **2**, 115 (1977)

[40] F. Barahona, R. Maynard, R. Rammal and J.P. Uhry, *J. Phys. A* **15**, 673 (1982).

[41] A. Hartwig, F. Daske and S. Kobe, *Comp. Phys. Commun.* **32**, 133 (1984)

[42] T. Klotz and S. Kobe, *J. Phys. A: Math. Gen.* **27**, L95 (1994)

[43] C. De Simone, M. Diehl, M. Jünger, P. Mutzel, G. Reinelt and G. Rinaldi, *J. Stat. Phys.* **80**, 487 (1995)

[44] K.F. Pál, *Biol. Cybern.* **73**, 335 (1995)

[45] J.D. Claiborne, *Mathematical Preliminaries for Computer Networking*, Wiley, New York 1990

[46] W. Knödel, *Graphentheoretische Methoden und ihre Anwendung*, Springer, Berlin 1969

[47] M.N.S. Swamy and K. Thulasiraman, *Graphs, Networks and Algorithms* (Wiley, New York 1991)

[48] J.-C. Picard and H.D. Ratliff, *Networks* **5**, 357 (1975)

[49] J.L. Träff, *Eur. J. Oper. Res.* **89**, 564 (1996)

[50] R.E. Tarjan, *Data Structures and Network Algorithms*, Society for industrial and applied mathematics, Philadelphia 1983

[51] B.A. Berg, U.E. Hansmann, T. Celik, *Phys. Rev. B* **50**, 16444 (1994).